



On the pharmacokinetics of two inhaled budesonide/formoterol combinations in asthma patients using modeling approaches

K. Soulele^a, P. Macheras^{a,b}, V. Karalis^{a,c,*}

^a Department of Pharmacy, School of Health Sciences, National and Kapodistrian University of Athens, 157 84 Athens, Greece

^b Pharma-Informatics Unit of Research & Innovation Center ATHENA, 151 25 Maroussi, Greece

^c Institute of Applied and Computational Mathematics (IACM), Foundation of Research and Technology Hellas (FORTH), Greece



ARTICLE INFO

Keywords:

Budesonide
Formoterol
Pharmacokinetic modeling
Asthma

ABSTRACT

Dry powder inhalers containing the budesonide/formoterol combination have currently a well-established position among other inhaled products. Even though their efficacy mainly depends on the local concentrations of the drug they deliver within the lungs, their safety profile is directly related to their total systemic exposure. The aim of the present investigation was to explore the absorption and disposition kinetics of the budesonide/formoterol combination delivered via two different dry powder inhalers in asthma patients. Plasma concentration–time data were obtained from a single-dose, crossover bioequivalence study in asthma patients. Non-compartmental and population compartmental approaches were applied to the available datasets. The non-compartmental analysis allowed for an initial characterization of the primary pharmacokinetic (PK) parameters of the two inhaled drugs and subsequently the bioequivalence assessment of the two different dry powder inhalers. The population pharmacokinetic analysis further explored the complex absorption and disposition characteristics of the two drugs. In case of inhaled FOR, a five-compartment PK model including an enterohepatic re-circulation process was developed. For inhaled BUD, the incorporation of two parallel first-order absorption rate constants (fast and slow) for lung absorption in a two-compartment PK model emphasized the importance of pulmonary anatomical features and underlying physiological processes during model development. The role of potential covariates on the variability of the PK parameters was also investigated.

1. Introduction

Inhalation therapy is widely used in the treatment of asthma, as it allows the delivery of relatively small doses of drugs directly to the site of action, achieving high local concentrations, whilst at the same time minimizing systemic adverse effects [1]. Fixed combination inhalers, including dry powder inhalers (DPIs) and pressurized metered dose inhalers (pMDIs), containing both an inhaled corticosteroid and a β_2 -adrenergic agonist have currently gained an established position among the recommended treatment options of asthma. In particular, DPIs containing the budesonide (BUD)/formoterol (FOR) combination, have played a central role in the management of moderate-to-severe asthma and other pulmonary diseases. Numerous randomized, double-blind clinical studies have shown this inhaled combination to be more

effective than each drug alone in improving airway function, controlling asthma symptoms, and reducing the risk of exacerbations; thus, providing a favorable therapeutic ratio compared to other treatment options [2,3].

Budesonide, is one of the most commonly used inhaled corticosteroids, with a proven efficacy record and a well-known safety profile. It acts by decreasing airway hyper-responsiveness and the number of inflammatory cells and mediators present in the airways of patients with asthma, treating not only the symptoms of asthma, but also the underlying cause of the disease [4]. The safety and efficacy profiles of inhaled BUD reflect the associated pharmacokinetic (PK) and pharmacodynamic properties [5]. In the literature there are studies that describe the BUD plasma levels after inhaled administration [6], however, relatively few studies have identified its pulmonary absorption and

Abbreviations: AIC, akaike information criterion; ANOVA, analysis of variance; BE, bioequivalence; BIC, bayesian information criterion; BMI, body mass index; BSV%, percent between subject variability; BUD, budesonide; CV%, percent coefficient of variation; DPI, dry powder inhaler; EHC, enterohepatic circulation; F, fraction of bioavailable dose; FEV1, forced expiratory volume exhaled in 1 s; FOR, formoterol; GB, gallbladder; GI, gastrointestinal; GMR, geometric mean ratio; IOV, inter-occasion variability; IPRED, individual predicted concentrations; IWRES, individual weighted residuals; LLOQ, lower limit of quantitation; ODE, ordinary differential equation; PULMO, Pulmoton® Elpenhaler®; RSE%, percent relative standard error; R, reference product; SYMBI, Symbicort® Turbuhaler®; SD, standard deviation; T, test product; VPC, visual predictive check

* Corresponding author. Laboratory of Biopharmaceutics - Pharmacokinetics, Department of Pharmacy, School of Health Sciences, National and Kapodistrian University of Athens, 157 84 Athens, Greece.

E-mail addresses: ksoulele@pharm.uoa.gr (K. Soulele), macheras@pharm.uoa.gr (P. Macheras), vkalis@pharm.uoa.gr (V. Karalis).

<https://doi.org/10.1016/j.pupt.2017.12.002>

Received 25 July 2017; Received in revised form 27 October 2017; Accepted 5 December 2017

Available online 06 December 2017

1094-5539/© 2017 Elsevier Ltd. All rights reserved.

systemic disposition characteristics. Inhaled budesonide reaches the systemic circulation either by direct absorption through the lungs or via gastrointestinal (GI) absorption of the drug that is inadvertently swallowed. Since BUD is a moderately lipophilic compound, it undergoes rapid uptake into the airway mucosa [7], while evidence suggests that fatty acid conjugates of the drug are formed and retained within the lung on inhalation, providing a slow-release depot of free drug [8]. This reversible esterification process has been shown to prolong the anti-inflammatory activity of BUD, allowing for a once-daily treatment regimen [4].

Formoterol is a highly potent, selective β_2 -adrenoceptor agonist, with a rapid onset and prolonged duration of bronchodilatory action. Following inhalation, the drug causes relaxation of the bronchial smooth muscles and pulmonary artery vasodilation, improves airway muscle function, and increases mucus clearance [3]. A significant bronchodilatory effect is already detected at 1 min after inhalation of a therapeutic dose which persists for at least 12 h. Formoterol has a predictable adverse event profile, including headache, tremor, palpitations, and decreased serum potassium, which is directly related to its total systemic exposure [9]. The drug has been shown to demonstrate complex absorption and distribution characteristics, i.e., absorption from different sites, enterohepatic recirculation, etc. [9]. However, its systemic time course following inhalation has not been adequately described, due to the very low (in the level of pg/mL) concentrations reached following inhalation of therapeutic doses, and PK data of formoterol in plasma or blood of humans are sparse in the literature [6,9,10].

The aim of the present investigation was, therefore, to explore the absorption and disposition kinetics of the BUD/FOR inhaled combination delivered via the single-dose DPI Pulmoton[®] Elpenhaler[®] (400/12 μ g/inhalation, ELPEN Pharmaceuticals) compared with the multi-dose DPI Symbicort[®] Turbuhaler[®] (400/12 μ g/inhalation, AstraZeneca) in asthma male and female patients. For this purpose, concentration (C) - time (t) data, obtained from a bioequivalence (BE) study with the two dry powder inhalers, were analyzed using non-compartmental and population compartmental approaches. The non-compartmental analysis was implemented for the initial characterization of the rate and extent of systemic exposure of inhaled BUD and FOR. Nevertheless, the main goal of this study was to apply population PK modeling in order to investigate the complex absorption and disposition characteristics of the two drugs following inhalation, as well as to determine the role of potential covariates on the variability of PK parameters. The description of pharmacokinetics of inhaled drugs is much more complicated than that of other routes of administration, as it requires the development of relatively simple mathematical schemes that can adequately represent the complex underlying physiologic processes following inhalation.

2. Materials and methods

2.1. Study design and volunteers

Plasma C-t data of budesonide and formoterol were obtained from a single-dose, two-sequence, two-period, crossover 2x2 BE study using two fix combination dry powder inhalers: Symbicort[®] Turbuhaler[®] (Budesonide/Formoterol 400/12 mcg/inhalation, AstraZeneca) and Pulmoton[®] Elpenhaler[®] (Budesonide/Formoterol 400/12 mcg/inhalation, ELPEN Pharmaceuticals), under fasting conditions. The study was performed in controlled and partly controlled asthma patients, while activated charcoal was co-administered, with a certain scheme, in order to prevent absorption of the two drugs from the gastrointestinal tract. A washout period of 6 days was set between the two treatment periods, in order to ensure the complete removal of the drugs from the body and prevent any carry-over effect during the second study period. The study was in compliance with the ICH E6 Good Clinical Practice Guidance and was conducted according to the principles of Helsinki Declaration. It was approved by the Romanian National Ethics Committee (approval

no: 1478;2050;2158 dated 7 July 2011) and the competent regulatory authorities (approval no: 25340E dated 11 July 2011). The trial was registered to the European Union Drug Regulatory Authorities Clinical Trials database (Eudra CT No: 2011-000614-19).

One hundred controlled or partly controlled asthma patients, according to the Global Initiative for Asthma (GINA) 2009 classification of Level Asthma Control [11], with mild to moderate exacerbations at medical history, were enrolled in the study. All subjects were informed about the purpose and potential risks of the study, and a written consent form was obtained by each study participant before enrollment. Male and female patients were considered eligible for inclusion in the study, if they met the following criteria: age between 18 and 65 years, body mass index (BMI) within 18.5–30 kg/m², no intolerance or hypersensitivity to study drugs, lactose or other milk proteins, absence of cardiovascular or other than respiratory disease, non-pregnant and non-lactating women. In subjects qualified for regular controller asthma therapy, normal asthma therapy was kept constant throughout the entire study period, except if they had been treated with the study drug combination. In the latter case, patients had to switch to an equivalent treatment at least 1 week before the initiation of the study. All participants had to be medication-free for at least 12 h and salbutamol-free for 6 h before study initiation. Patients were excluded from the study if they had poor asthma control and frequent exacerbations in the past year, participation in another clinical trial in the last three months, hospitalization or donation of ≥ 450 mL of blood within two months prior to study initiation, upper respiratory tract infection or history of other relevant pulmonary disease, renal or hepatic insufficiency, positive AIDS or hepatitis B/C tests results, and alcohol or drug abuse. Vital signs measurements and clinical examinations were performed before and after the study drugs administration in each study period, and all reported adverse effects were recorded and evaluated.

On the treatment days, after at least 8 h of fasting, each subject received either one dose of Pulmoton[®] Elpenhaler[®] 400/12 mcg/inhalation ("PULMO", test formulation) or one dose of Symbicort[®] Turbuhaler[®] 400/12 mcg/inhalation ("SYMBI", reference formulation), according to the randomization scheme. An activated charcoal scheme was administered 2 min pre-dosing, and at 2 min, 1, 2 and 3 h post-dose in order to block any absorption from the gastrointestinal tract. Blood samples (of 6 mL) were collected before drug administration (time 0) and at 1, 3, 5, 10, 15, 30, 45 min and 1, 1.33, 1.67, 2, 2.33, 2.67, 3, 4, 5, 6, 8, 12, 16, 24, 36, and 48 h post-dose. Following the six days of washout period, patients received the alternate formulation and the same procedures were followed, as in the first study period.

2.2. Assay methodology

The quantification of FOR was performed in all the collected plasma samples up to 48 h post-dose, whereas BUD plasma concentrations were determined up to 24 h. Two separate Liquid Chromatography/Mass Spectrometry (LC-MS/MS) methods were developed and applied for the analysis of each drug which were firstly presented in a previous study [6]. Both analytical techniques were validated and presented adequate sensitivity, precision, accuracy, specificity, and linearity. The lower limits of quantification were 5.000 pg/mL for BUD and 0.300 pg/mL for FOR [6].

2.3. Pharmacokinetic analysis

2.3.1. Non-compartmental pharmacokinetic analysis

Budesonide and formoterol C-t data were, initially, analyzed using non-compartmental methods and the following PK parameters were calculated: the area under the concentration-time curve from time zero to the last quantifiable sample (AUC_t) using the linear trapezoidal rule, the first recorded maximum plasma concentration value (C_{max}), the time at which C_{max} occurs (T_{max}), and the area under the C-t curve from time zero extrapolated to infinity (AUC_{inf}). Descriptive statistics were

also calculated for these PK parameters.

Bioequivalence assessment was also performed on the primary PK parameters (AUC_t and C_{max}) following the current methodology proposed by the European Medicines Agency [12]. The ninety percent confidence intervals (90% CI) around the geometric mean ratios (GMR) of T over R formulation (T/R) were constructed. The two inhalers were considered bioequivalent if the 90% CIs for the log-transformed values of both AUC_t and C_{max} were lying within the pre-determined equivalence range of 80–125% for both active agents [12]. The entire analysis was implemented in WinNonlin® v.5.0.1 (Pharsight Corp, Menlo Park, CA).

2.3.2. Population pharmacokinetic analysis

Data for both drugs were further analyzed using a compartmental population PK methodology. A non-linear mixed effects model approach was applied separately for each drug and the entire computational work has been implemented in Monolix® 2016R1 software (Lixoft, Orsay France). Since in the present study the C-t data derived from a crossover BE study, data for each drug obtained from the different treatment periods and administered products (PULMO and SYMBI) were pooled together setting ‘period’ and ‘treatment’ effects as potential covariates in the final dataset. Similar methodologies in the treatment of data and population analysis have been suggested in previous published works [13–15]. Finally, a dose of 320 mcg instead of 400 mcg was considered for BUD and 9mcg instead of 12mcg for FOR. The latter correction was in accordance with the relevant drug products information, since these two doses (i.e., 320 mcg and 9 mcg) are the actually delivered doses through the mouthpiece during inhalation [16].

Initially, the analysis focused on the selection of the most appropriate structural model for each drug and thus, typical one-, two-, and three-compartment models with different drug input kinetics were investigated. However, since both drugs (BUD and FOR) exhibited rather complex PK profiles following inhaled administration, conventional models were proven inadequate to describe the kinetics of the two drugs and structural models of increasing complexity had to be constructed. The developed models were encoded through an ordinary differential equation (ODE) system in the model translator MLXTRAN of Monolix® software.

In particular, in the case of FOR a small plateau or a second lower peak was observed at around 4 h post-dose in the majority of C-t profiles. Since an activated charcoal scheme was administered up to 3 h in the present study, gastrointestinal absorption of the swallowed part of the inhaled dose was excluded, and the observed second peak was attributed to an enterohepatic circulation (EHC) process, known to occur in the case of FOR. For this reason, PK models capable of describing this re-distribution process within the body were developed. Different scenarios were tested, including multi-compartment models with bile and GI compartments, addition of an enterohepatic loop using bolus, first- or zero-order kinetics between compartments, sine function models for gallbladder emptying control providing oscillatory enterohepatic circulation, different lag time periods for gallbladder emptying, presence or absence of fecal elimination, etc. Absorption from the lungs, as well as elimination from the central and/or GI compartments were assumed to follow first-order kinetics.

Similarly, BUD also required the development of a more complex PK model, in order to describe its multiphasic lung absorption characteristics. The choice of two parallel lung absorption processes for BUD has been also previously suggested by Weber and Hochhaus [17]. A parallel fast and slow pulmonary absorption process was, therefore, incorporated in the PK model. Single- or double-input processes, pulmonary depot sub-compartments, transit absorption compartment models with first- and zero-order rate constants, Erlang-type transit compartments, and time-dependent absorption were also evaluated. Accordingly, oral absorption was excluded due to the co-administration of the activated charcoal scheme. One-, two-, and three-compartment

models, were investigated for the distribution kinetics of BUD. In all cases, elimination was considered to take place in the central compartment and follow first-order kinetics.

The between-subject variability (BSV) was assumed to follow log-normal distribution for all PK parameters of FOR. In case of BUD, in addition to log-normal distribution, a logit-transformation was also implemented in certain PK parameters constrained to be on a zero to one scale. The variability in PK parameters between the different study periods (“inter-occasion variability” or “IOV”) was also evaluated, while the possibility of correlation between the random effects of the PK parameters was also assessed. Various statistical models (constant, proportional, exponential, and combined) describing the random residual variability of the structural models were considered.

Following the determination of the best structural model for each drug, various covariates were tested for their contribution in the model, including: body weight, gender, age, height, body mass index (BMI), asthma disease state, and baseline FEV1 (forced expiratory volume exhaled in 1 s) measurements. Allometric scaling with body weight as the size descriptor and fixed exponents (1 for the volume of distribution and 0.75 for clearance) was also assessed. The effects of the administered DPI formulations (‘treatment’) and the treatment period (‘occasion’) were also assessed as potential covariates. In all cases, the continuous covariates were examined either untransformed or centered around their ‘mean’ value. A combination of forward addition and backward elimination methods was implemented for the investigation of all potential covariates, and the effect of each covariate on reducing the numerical selection criteria, the between-subject-variability (BSV) of the PK parameters and the obtained p value were evaluated.

Candidate models for BUD and FOR were assessed in terms of model statistics and numerical criteria, as well as visual inspection of goodness-of-fit plots and simulation-based diagnostics. PK parameter estimates were required to be physiologically plausible and had to remain stable when significant digits and initial parameter estimates were altered. With respect to the visual inspection, (a) the adequacy of fitting of the model predicted estimates to the actual C-t data was evaluated for each model, (b) individual and population predicted plasma concentrations were directly compared to the observed data, (c) the amount of bias was assessed by plotting the individual weighted residuals (IWRES) versus the individual predicted (IPRED) concentrations, and (d) distributions of random effects were compared to the theoretical normal. The ability of the model to simulate data in line with the observed data was finally assessed with visual predictive check (VPC) plots.

3. Results

Finally, 90 subjects were included in the non-compartmental and population PK analyses since ten volunteers withdrew from the study. A number of 59% of the enrolled subjects had controlled asthma. Three subjects were considered as dropouts referring to positive pregnancy test results and seven patients presented very low or undetectable plasma drug levels in the majority of their samples. The demographic characteristics of the enrolled subjects along with their descriptive statistics are listed in Table 1. Forty-three non-serious adverse events (headache, vomiting and dizziness) were recorded in the study: 32 of moderate and 11 of mild intensity were equally distributed between the two treatments [6]. No deaths or any other significant adverse events were recorded and all volunteers completely recovered before the termination of the study.

3.1. Non-compartmental pharmacokinetic analysis

The observed mean plasma concentrations of FOR and BUD versus time, following a single inhaled dose from PULMO and SYMBI, are presented in Fig. 1A and B, respectively. Despite the increased variability following inhaled administration, quite similar drug C-t profiles

Table 1
Descriptive statistics of demographic characteristics of the enrolled subjects.

	Age (years)	Weight (Kg)	Height (cm)	BMI ^a (Kg/m ²)
Mean	46.85	73.26	166.61	26.40
SD ^b	11.51	11.50	9.03	3.59
CV % ^c	24.6	15.7	5.4	13.6
Minimum	19	50	150	18.7
Maximum	65	97	192	30.0
Range	46	47	42	11.3

^a Body mass index.
^b Standard deviation.
^c Percent coefficient of variation.

were obtained for the two DPI products.

The calculated mean PK parameters (i.e. AUC_t, AUC_{inf}, C_{max}, T_{max}, and λ_z) accompanied by their statistical descriptive criteria are summarized in Table 2 for FOR and Table 3 for BUD. Comparable values between the two tested formulations were obtained for C_{max}, AUC_t and AUC_{inf} for both drugs. The derived CV% values ranged from 25.6 to 47.9% for the estimated PK parameters of FOR and from 37.9 to 64.5% for PK parameters of BUD (Tables 2 and 3).

The primary PK parameters, C_{max} and AUC_t, for BUD and FOR were further analyzed following the BE assessment methodology of the EMA guideline [12]. For both drugs, the percent GMRs of C_{max} and AUC_t estimates, along with the 90% CIs are within the acceptance range of 80–125%, indicating that the two products are bioequivalent (Tables A1 and A2 in the Appendix).

3.2. Population pharmacokinetic analysis

In total, 180 (= 2 periods x 90 patients) C-t profiles were used for the population PK analysis and model building of each drug. As

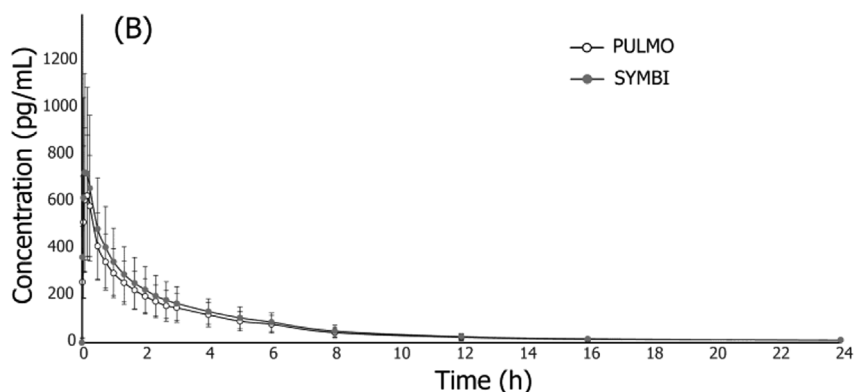
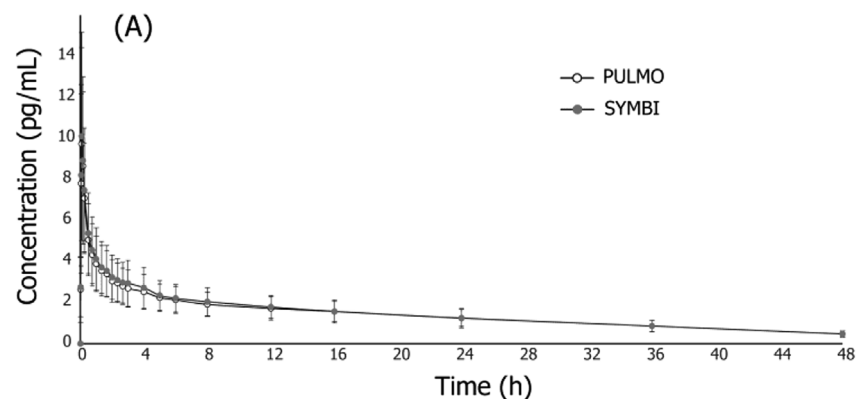


Fig. 1. Mean plasma concentration - time profiles of formoterol (A) and budesonide (B) for the test (PULMO) and reference (SYMBI) dry powder inhalers. The error-bars refer to the standard deviation of the concentration values at each time-point.

Table 2
Pharmacokinetic (PK) parameters and statistical descriptive criteria for the plasma concentration-time data of inhaled formoterol (reference and test products) in 90 asthma patients.

PK parameter ^a	Mean	SD ^b	CV% ^c	Median	Min	Max
SYMBI (reference)						
AUC _t (pg/mL/h)	69.417	19.729	28.4	68.018	21.805	117.249
C _{max} (pg/mL)	10.356	4.962	47.9	9.288	2.272	33.977
AUC _{inf} (pg/mL/h)	83.513	21.703	26.0	81.787	35.840	148.372
T _{max} (h)	–	–	–	0.083	0.05	0.5
λ _z (h ⁻¹)	0.040	0.010	25.6	0.040	0.016	0.065
PULMO (test)						
AUC _t (pg/mL)	67.523	20.666	30.6	69.632	26.141	145.293
C _{max} (pg/mL)	10.117	4.630	45.8	8.86	3.371	25.797
AUC _{inf} (pg/mL/h)	81.432	22.831	28.0	81.728	35.106	173.926
T _{max} (h)	–	–	–	0.083	0.05	0.5
λ _z (h ⁻¹)	0.040	0.010	25.8	0.040	0.016	0.069

^a AUC_t: area under the concentration-time curve from time zero to the last quantifiable sample; C_{max}: the first recorded maximum plasma concentration value; AUC_{inf}: area under the concentration-time curve from time zero extrapolated to infinity; T_{max}: the time at which C_{max} occurs; λ_z: apparent terminal elimination rate constant.
^b Standard deviation.
^c Percent coefficient of variation.

reported in the ‘Methods’ section, both FOR and BUD presented complex absorption and disposition kinetics following inhaled administration, with the classic one-, two- and three-compartment models proven inadequate to describe the available C-t data. Therefore, MLXTRAN codes were developed for each drug and further assessed for their performance.

3.2.1. Formoterol

In the case of FOR, visual inspection of the individual C-t profiles

Table 3

Pharmacokinetic (PK) parameters and statistical descriptive criteria for the plasma concentration-time data of inhaled budesonide (reference and test products) in 90 asthma patients.

PK parameter ^a	Mean	SD ^b	CV% ^c	Median	Min	Max
SYMBI (reference)						
AUC _t (pg/mL/h)	1769.415	759.655	42.9	1613.058	191.131	4159.821
C _{max} (pg/mL)	818.993	411.144	50.2	800.775	109.588	2214.556
AUC _{inf} (pg/mL/h)	1844.653	789.637	42.8	1690.863	208.889	4366.584
T _{max} (h)	–	–	–	0.167	0.05	1.00
λ _z (h ⁻¹)	0.169	0.064	37.9	0.162	0.056	0.343
PULMO (test)						
AUC _t (pg/mL)	1541.628	617.343	40.1	1406.357	478.144	3366.919
C _{max} (pg/mL)	709.483	277.298	39.1	725.356	182.660	1568.544
AUC _{inf} (pg/mL/h)	1614.704	655.631	40.6	1454.959	523.423	3579.876
T _{max} (h)	–	–	–	0.167	0.05	1.00
λ _z (h ⁻¹)	0.180	0.116	64.50	0.166	0.060	0.984

^a AUC_t: area under the concentration-time curve from time zero to the last quantifiable sample; C_{max}: the first recorded maximum plasma concentration value; AUC_{inf}: area under the concentration-time curve from time zero extrapolated to infinity; T_{max}: the time at which C_{max} occurs; λ_z: apparent terminal elimination rate constant.

^b Standard deviation.

^c Percent coefficient of variation.

(Fig. 2) revealed a plateau or second smaller concentration peak within 3–5 h post-dose.

The contribution of absorption of the swallowed fraction of dose from the GI tract was excluded due to the concomitant administration of activated charcoal; thus, the second peak is most probably attributed to an enterohepatic recirculation of FOR. In our analysis, inhaled FOR kinetics was best described by a structural model consisting of a two-compartment disposition model linked to a lung compartment, as well as to serial gallbladder (GB) and gastrointestinal (GI) compartments for the description of the EHC process (Fig. 3).

In the EHC loop, the two additional compartments (i.e., GB and GI) were linked by first-order kinetics and a gallbladder emptying time interval, based on the time of the second peak observed in the C-t plot, i.e. between 2 and 5 h post-dose. The EHC process was modeled by introducing a first-order rate constant (K_b) describing the drug transfer from the central compartment to the GB compartment. When gallbladder emptying occurred, FOR was introduced to the GI compartment and was reabsorbed into the central compartment. First-order absorption from the GI compartment was initiated at 3 h post-dose, since then was the termination of the co-administered activated charcoal scheme. Elimination was considered, for both the central and the GI compartments, to follow first-order kinetics.

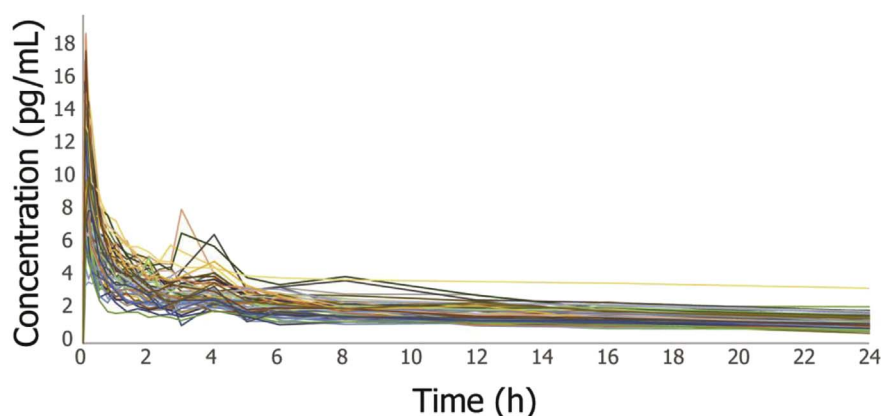


Fig. 2. Individual concentration-time profiles of FOR in plasma of 90 asthma patients after a single inhaled dose of formoterol fumarate from two dry powder inhalers.

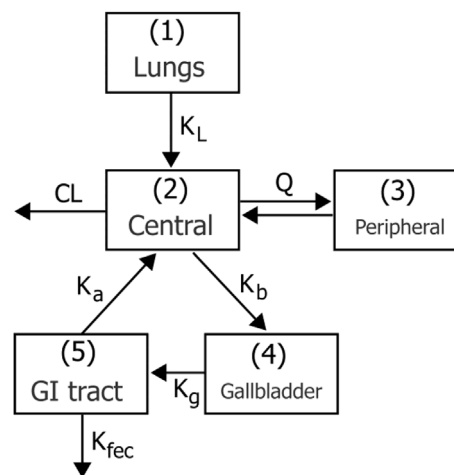


Fig. 3. Schematic diagram of the final two-compartment model used to describe the pharmacokinetics of FOR after inhalation with activated charcoal. Compartments: lung compartment (1), central compartment (2), peripheral (3), gallbladder (4) and gastrointestinal compartment (5) for the enterohepatic re-circulation process. Key: K_L = first-order absorption rate constant from the lungs (h⁻¹); Q = inter-compartmental clearance of the drug (L/h); K_b = transfer rate constant to the gallbladder (h⁻¹); K_g = excretion rate constant from gallbladder to the intestine (h⁻¹); K_a = absorption rate constant from the gastrointestinal tract (h⁻¹); K_{fec} = fecal elimination rate constant (h⁻¹); CL = clearance from the central compartment (L/h).

The population parameter estimates of the final PK model of FOR, along with the BSV% and RSE% values are listed in Table 4.

The PK estimates of the final best model were the following: absorption rate constant through the lungs (K_L) = 14.8 h⁻¹, apparent volume of distribution of the central compartment (V_c/F) = 619 L, apparent volume of distribution of the peripheral compartment (V_p/F) = 1130 L, apparent clearance from the central compartment (CL/F) = 93 L/h, inter-compartmental clearance (Q/F) = 2350 L/h, transfer rate constant from the central compartment to bile (K_b) = 0.37 h⁻¹, excretion rate constant from the gallbladder to the intestine (K_g) = 0.7 h⁻¹, GI absorption rate constant (K_a) = 0.26 h⁻¹, and fecal elimination rate constant (K_{fec}) = 0.01 h⁻¹. It is reasonable that only “apparent” PK parameters could be estimated in the present study, since only inhaled administration was performed and not intravenous administrations. For this reason, the term F was included, referring to the bioavailable fraction of dose. BSV% estimates were found to exhibit moderate to high values, which ranged approximately from 15% to 88%. The RSE% values, obtained for both PK and BSV% estimates, were relatively low (3–23%), indicating that the model parameters were precisely estimated (Table 4).

The residual error model that led to the optimum performance was a combined error model consisting of an additive component *a* and multiplicative coefficient *b*:

Table 4

Population parameters for the final best PK model applied to the formoterol data. Key: PK = pharmacokinetic; K_L = first-order absorption rate constant from the lungs (h^{-1}); V_c/F = apparent volume of drug distribution (L) of the central compartment; V_p/F = apparent volume of drug distribution (L) of the peripheral compartment; Q/F = apparent inter-compartmental clearance of the drug (L/h); CL/F = apparent clearance from the central compartment (L/h); K_b = transfer rate constant to the gallbladder (h^{-1}); K_g = excretion rate constant from gallbladder to the intestine (h^{-1}); K_a = absorption rate constant from the gastrointestinal tract (h^{-1}); K_{fec} = fecal elimination rate constant (h^{-1}); F = fraction of bioavailable dose; a and b = residual error parameters for the combined error model (Eq. (1)); RSE% = relative standard error of the calculation of the population pharmacokinetic estimate; BSV% = between subject variability.

Parameter	Mean (RSE%)	BSV% (RSE%)
K_L (h^{-1})	14.8 (3)	15.08 (23)
V_c/F (L)	619 (4)	32.30 (14)
V_p/F (L)	1130 (4)	36.65 (10)
Q/F (L/h)	2350 (6)	48.89 (10)
CL/F (L/h)	93 (3)	24.66 (9)
K_b (h^{-1})	0.37 (5)	48.31 (8)
K_g (h^{-1})	0.70 (8)	61.83 (15)
K_a (h^{-1})	0.26 (6)	48.89 (13)
K_{fec} (h^{-1})	0.01 (14)	88.42 (20)
PK Random Effects Correlation		
$V_p/F - Q/F$	0.74 (11)	-
Residual error model		
a	0.12 (7)	-
b	0.15 (2)	-

$$C_{ij} = f_{ij} + (a + b \cdot f_{ij}) \cdot \varepsilon_{ij} \quad (1)$$

where C_{ij} is the j th observed concentration of FOR for the i th individual, a and b are the parameters of the residual error model, f_{ij} is the j th model predicted value for i th subject, and ε_{ij} is the random error which is assumed to be normally distributed with mean 0 and variance 1. The residual error parameters for the combined error model (Eq. (1)) were: $a = 0.12$ and $b = 0.15$. Finally, a significant correlation of the random effects between the two PK parameters, V_p/F and Q/F ($\text{corr} = 0.74$) was incorporated in the final model, as it lead to better fittings and improved numerical criteria. No effect of gender, age, body weight, height and BMI on FOR estimated PK parameters was found, and no difference in the performances of the two DPIs, or between the different treatment periods was observed.

3.2.2. Budesonide

For BUD, the final best model was obtained when a two-compartment disposition model was connected with two lung absorption compartments (Fig. 4).

In this case, in order to account for the two parallel first-order absorption processes, the lung was composed of two absorption compartments to describe the 'fast' and 'slow' absorption of inhaled BUD. Elimination was assumed to take place in the central compartment following first-order kinetics. Table 5 summarizes the estimates of the population parameters of the final model, along with their BSV% and RSE% values.

The structural PK model was parameterized in terms of the fast ($K_{\text{af}} = 19.7 \text{ h}^{-1}$) and slow ($K_{\text{as}} = 0.11 \text{ h}^{-1}$) lung absorption rate constants, the relative fraction of dose absorbed slowly ($R_{\text{s}} = 0.67$) through the lungs and the $R_{\text{fast}}/R_{\text{slow}}$ ratio ($z = R_{\text{fast}}/R_{\text{slow}} = 0.27$), where R_{fast} refers to the fraction of dose absorbed rapidly through the lungs. Besides, the remaining model parameters are the apparent volume of distribution in the central ($V_c/F = 228 \text{ L}$) and peripheral ($V_p/F = 182 \text{ L}$) compartments, the apparent inter-compartmental clearance ($Q/F = 254 \text{ L/h}$), and the apparent clearance ($CL/F = 154 \text{ L/h}$). A combined additive and proportional error model (Eq. (1)) was used to

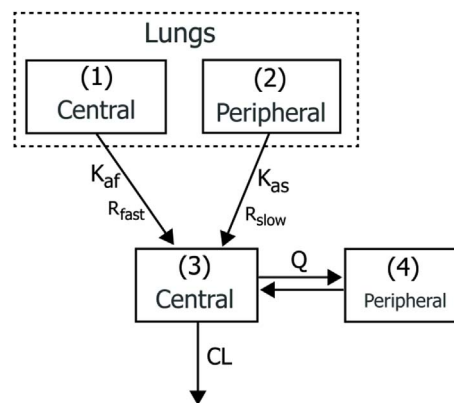


Fig. 4. Schematic diagram of the final two-compartment model used to describe the pharmacokinetics of BUD after inhalation with activated charcoal. Compartments: central lung compartment (1), peripheral lung compartment (2), central compartment (3), peripheral compartment (4). Two different first-order input rates (fast and slow) were considered for lung absorption of inhaled BUD, with a relative fraction of the inhaled dose (R_{fast}) absorbed rapidly via the lungs and another fraction (R_{slow}) showing a delayed absorption. Key: K_{af} = fast first-order absorption rate constant from the lungs (h^{-1}); K_{as} = slow first-order absorption rate constant from the lungs (h^{-1}); R_{fast} = relative fraction of dose absorbed rapidly from the lungs; R_{slow} = relative fraction of dose absorbed slowly from the lungs; Q = apparent inter-compartmental clearance of the drug (L/h); CL = apparent clearance from the central compartment (L/h).

Table 5

Population parameters for the final PK model applied to the budesonide data. Key: PK = pharmacokinetic; K_{af} = fast first-order absorption rate constant from the lungs (h^{-1}); K_{as} = slow first-order absorption rate constant from the lungs (h^{-1}); R_{slow} = relative fraction of dose absorbed slowly from the lungs; z = the ratio of dose fractions absorbed either fast (R_{fast}) or slowly (R_{slow}) through the lungs (i.e. $R_{\text{fast}}/R_{\text{slow}}$); V_c/F = apparent volume of drug distribution (L) of the central compartment; V_p/F = apparent volume of drug distribution (L) of the peripheral compartment; Q/F = apparent inter-compartmental clearance of the drug (L/h); F = fraction of bioavailable dose; a and b = residual error parameters for the combined error model (Eq. (1)); RSE% = relative standard error of the calculation of the population pharmacokinetic estimate; BSV% = between subject variability.

Parameter	Mean (RSE%)	BSV% (RSE%)
K_{af} (h^{-1})	19.7 (8)	72.34 (12)
K_{as} (h^{-1})	0.11 (11)	51.38 (12)
R_{slow}	0.67 (3)	63.75 (17)
z	0.27 (5)	49.72 (11)
V_c/F (L)	228 (3)	28.24 (10)
V_p/F (L)	182 (6)	35.77 (10)
Q/F (L/h)	254 (6)	50.90 (10)
CL/F (L/h)	154 (3)	22.79 (9)
PK Random Effects Correlation		
$K_{\text{af}} - R_{\text{slow}}$	0.45 (38)	-
$V_p/F - Q/F$	0.84 (6)	-
Covariates effects		
Gender on K_{as}^a	-0.58 (23) ($p = 1.6 \times 10^{-5}$)	-
Gender on V_p/F^a	0.22 (28) ($p = 0.00031$)	-
Residual error model		
a	0.90 (18)	-
b	0.13 (2)	-

^a Males were considered as the 'control' group.

describe the residual unexplained variability. The estimated residual error parameters were: $a = 0.90$ and $b = 0.13$. A significant correlation of the random effects between $V_p/F - Q/F$ ($\text{corr} = 0.84$) and $K_{\text{af}} - R_{\text{slow}}$ ($\text{corr} = 0.45$) was found and included in the final model. BSV% values

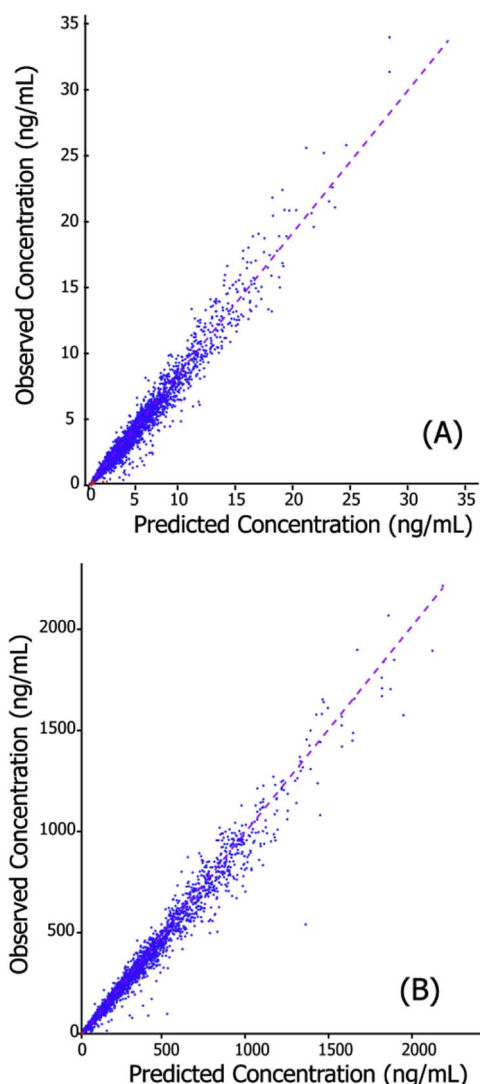


Fig. 5. Individual predicted concentrations from the population pharmacokinetic models versus the observed plasma concentration values of A) Formoterol and B) Budesonide. The diagonal dashed line represents the line of unity, namely, the ideal situation.

ranged from 22% to 72%, while RSE% values remained relatively low ranging from 9 to 17% for all the estimated parameters (Table 5).

Gender was found to be a significant covariate on K_{as} ($p = 1.6 \times 10^{-5}$) and V_p/F ($p = 0.00031$), with male subjects exhibiting a faster absorption for the slow lung absorption phase of BUD and lower peripheral distribution compared to females (Eqs. (2) and (3)). Besides, the inclusion of a gender effect on these two PK parameters led to significantly improved numerical criteria and fitting results of the final PK model.

$$K_{as} = \theta_1 \cdot \exp(-0.58) \quad (2)$$

$$V_p/F = \theta_2 \cdot \exp(0.22) \quad (3)$$

where θ_1 and θ_2 refer to the typical population PK parameter estimates for male subjects. No ‘treatment’, ‘period’ or any other covariate effect was found to be significant ($p > 0.05$) on any other PK parameter.

3.2.3. Goodness-of-fit plots

Goodness-of-fit plots for the final PK models of FOR and BUD are depicted in Figs. 5–7. Fig. 5A and B shows the individual predicted concentrations versus the observed concentration values for the final population PK models of FOR and BUD, respectively. A symmetric distribution of points around the line of unity is observed in both cases,

showing an adequate degree of linearity and a reasonable agreement between the predicted and observed concentrations for both PK models.

In line with the above, the weighted residuals (IWRES) versus the individual predictions, illustrated in Fig. 6 (A, B) for both models, also show a balanced distribution around the zero line, indicating that the combined (proportional and additive) error model provided adequate description of the residual error.

Finally, Fig. 7A and B represent the visual predictive check (VPC) plots obtained for each compound. The predictions from the model described adequately the observed high and median concentration profiles of both compounds, suggesting that the utilized structural/error models were appropriate for describing the plasma C-t profiles of FOR and BUD, respectively.

4. Discussion

The study aimed at investigating the pharmacokinetics of the inhaled combination BUD/FOR in an asthma patient group in order to elucidate the absorption and disposition characteristics of these two drugs. In this respect, a standard non-compartmental PK approach and a population PK modeling methodology were applied.

4.1. Non-compartmental pharmacokinetic analysis

The non-compartmental approach was applied initially to the available C-t data in order to get the estimates of some basic PK parameters. Even though low plasma drug levels were obtained in both cases (Fig. 1), the high sensitivity of the bioassays allowed the accurate quantification and characterization of the PK profiles of both FOR and BUD. It is worth mentioning that the C-t levels reflected solely the initial pulmonary absorption, since the gastrointestinal absorption of the swallowed fraction, following inhaled administration, has been blocked by the co-administration of an activated charcoal scheme [18].

Peak plasma concentrations of BUD were achieved within 30 min following inhalation, while the lung absorption of FOR was even faster with maximum drug concentrations in most subjects found within 5–10 min. Short absorption half-lives have been also reported for both drugs in previous studies in asthma patients and healthy volunteers [7,10]. This is in accordance with the moderately lipophilic character of both molecules, found to be readily dissolved in human bronchial secretions and rapidly absorbed across the lung epithelium [19,20]. The primary PK parameters of BUD and FOR were calculated separately for each DPI product (PULMO or SYMBI), and were further compared in terms of BE assessment, according to the currently proposed EMA methodology [12]. Even though a considerable debate on the use of BE studies to demonstrate similarity between two orally inhaled products exists, the simplicity and lack of controversy of performing PK studies compared with other methods, support the role of PK studies on ensuring substitutability of such generic products [18]. Particularly in cases where a drug substance exhibits negligible gastrointestinal bioavailability, or, as in our study, oral absorption can be prevented through an activated charcoal scheme, plasma PK studies are considered the most sensitive methodology for detecting formulation differences [21]. Besides, the additional application of PK modeling approaches based on data derived from PK studies may be also used as an alternative method for studying the pulmonary fate of the two inhaled products and serve as surrogate evidence in the demonstration of their bioequivalence [13,14,22].

4.2. Population pharmacokinetic analysis

Visual inspection of the plasma C-t profiles of BUD and FOR revealed rather complex absorption and distribution characteristics that could not be explained by the classic non-compartmental analysis. Pharmacokinetics of inhaled drugs is much more complicated than that of other routes of administration. In particular, certain physiological

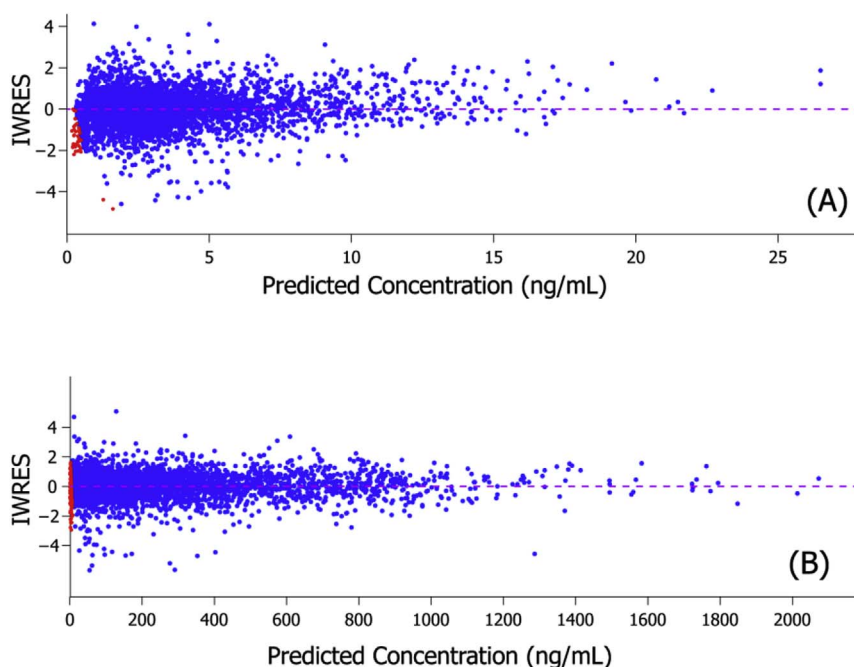


Fig. 6. Graphical representation of the individual weighted residuals (IWRES) versus the individual predicted concentrations (IPRED) for the final model of A) Formoterol and B) Budesonide. Points in red color refer to the missing data due to censoring. (For interpretation of the references to color in this figure legend, the reader is referred to the Web version of this article.)

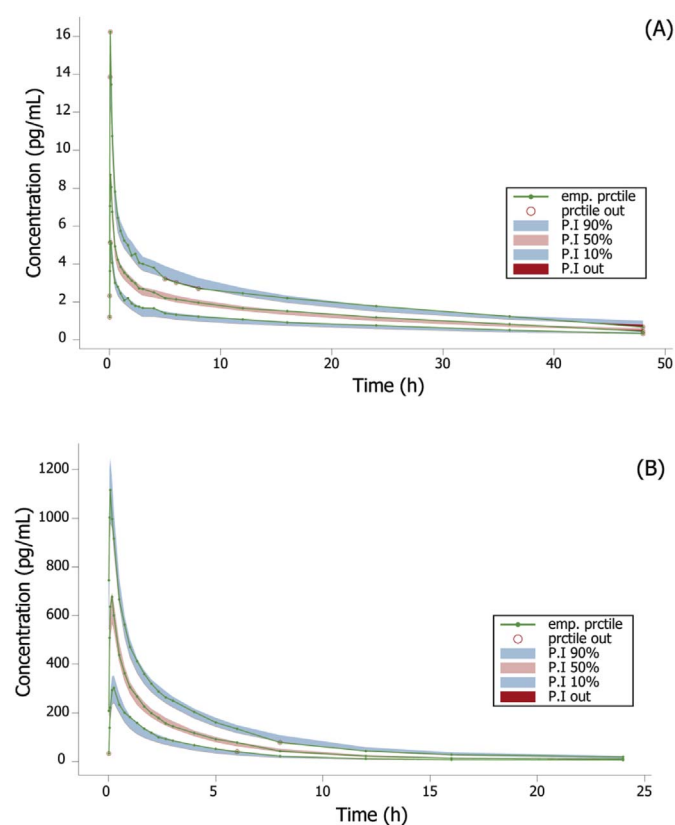


Fig. 7. Visual predictive check of the final model for: A) Formoterol and B) Budesonide. Key: solid lines refer to the 10th, 50th, and 90th percentiles of the empirical data; shaded areas refer to the 95% prediction intervals around each theoretical percentile.

parameters, such as the mucociliary clearance, lung deposition, differences in absorption between central and peripheral areas of the lung, as well as formulation characteristics (e.g., particle size, dissolution rate) or patient-related factors (e.g., health status, lung function) can significantly influence the PKs of these drugs [17]. For this reason, the primary aim of this study was to develop population PK models able to

describe the entire time profiles of inhaled BUD and FOR. A dataset of 180 individual C-t profiles were used for the development of the two structural PK models. Data for the two DPI products from each study period were combined, by considering the ‘period’ (i.e., occasion) and ‘treatment’ (i.e., PULMO or SYMBI) effects as potential covariates.

4.2.1. Formoterol

In case of FOR, inspection of the individual C-t profiles (Fig. 2) revealed either a plateau or small double concentration peaks, observed in most subjects between 3 and 5 h post-dose. These lesser peaks, observed at later times, were considered to reflect the enterohepatic re-circulation of the drug, since gastrointestinal absorption of the swallowed fraction was excluded due to the co-administration of activated charcoal. Besides, it has been previously reported that, apart from renal excretion, formoterol glucuronide conjugates might be excreted via the bile, into the intestinal lumen and subsequently cleaved by the gut flora, resulting in reabsorption of the free drug by enterocytes and re-circulation through the liver [9,23]. This finding was further supported by animal studies where, biliary excretion of FOR accounted for about 31–65% of an orally administered dose [24]. Therefore, an enterohepatic re-circulation model was developed for inhaled FOR in our study, based on the above-mentioned physiological aspects of biliary excretion and re-circulation processes. Plasma C-t profiles were best described by a five-compartment model capable of simulating the processes of lung absorption, systemic disposition, tissue distribution of the drug and gallbladder emptying during the enterohepatic recycling and subsequent intestinal absorption and elimination. The final structural model consisted of a two-compartment disposition model linked to a lung absorption compartment and sequential gallbladder and GI compartments representing the EHC loop (Fig. 3). For reasons of simplicity, the liver (as a well perfused organ) was considered part of the central compartment, while, metabolic and de-esterification reactions of FOR were omitted in the final model.

It should be mentioned that in actual physiological conditions, the EHC process is much more complicated and several PK models have been proposed for the proper characterization of the EHC process. Reported models for other drugs showing enterohepatic re-circulation either assumed continuous enterohepatic recirculation [25], one or multiple secretions of bile using an on/off switch time interval [26], time-dependent transfer from bile into gut [27], or implemented a sine

function to describe periodic bile releases [28]. When more complicated methodologies were implemented in our case, the model was over-parameterized and no reliable fits could be obtained. Nevertheless, in our study we investigated many of these possibilities.

Unlike conventional PK models, EHC models require the determination of additional rate parameters for the description of biliary excretion, intestinal absorption, fecal and urinary elimination of the active compound. Defining appropriate characteristics, such as the rate constants for the EHC loop, the 'lag-time' for the GI absorption and the gallbladder emptying time interval, was a key element during model construction. In our final model, the enterohepatic loop compartments were linked by first-order transport rate constants, while a lag-time of 3 h was considered for the initiation of GI absorption, due to the presence of activated charcoal. Finally, a gallbladder emptying time interval between 2 and 5 h post-dose was chosen, based on the observed secondary absorption peak in the individual plasma C-t profiles of FOR. Even in the absence of food, a partial discharge of gallbladder bile into the duodenum during the inter-digestive period could also be considered [29]. Northfield and Hofmann [30] have previously reported that there is a secretion of bile acids into the duodenum during the fasting state. During late phase II of the inter-digestive period, intragallbladder pressure increments favor flow of a small amount of bile into the bile duct and, through the sphincter of Oddi, into the duodenum [31].

The estimates of the population PK parameters for the final PK model, their BSV% and RSE% values are listed in Table 4. A high absorption rate constant ($K_L = 14.8 \text{ h}^{-1}$) was estimated for FOR, which is in accordance with the small T_{\max} values (5–10 min) observed in the non-compartmental analysis, while the apparent volumes of distribution for the central ($V_c/F = 619 \text{ L}$) and the peripheral compartments ($V_p/F = 1130 \text{ L}$) were in line with the moderately lipophilic character of the drug and in agreement with previously reported values [10,32]. Clearance of the drug from the central compartment ($CL/F = 93 \text{ L/h}$) was determined to be somewhat smaller compared with other reported values [10], which may be partly explained by the addition of fecal elimination contributing to the total clearance of the drug. A moderate inter-individual variability was observed for most PK parameters of FOR. However, rate constants between the central and peripheral compartments and within the EHC loop varied largely within the study population, highlighting the increased inter-subject variability in the re-distribution processes.

In regards to the covariate model, no significant correlation was observed between the examined covariates and the PK parameters of FOR. Demographic characteristics, the effect of inhalation device, treatment period, and patient status were not found to influence systemic drug exposure of FOR. The goodness-of fit results (Figs. 5A, 6A and 7A) showed that the model was able to provide sensible predictions of the observed values despite some difficulties in capturing the EHC of FOR in some individuals and the increased variability attributed to the large sample size of the study population and the complexity of the EHC process.

4.2.2. Budesonide

At 10–15 min after BUD inhalation, a peak serum concentration was observed with a subsequent slower elimination of the drug (Fig. 1B). The initial absorption phase was considered to reflect a rapid absorption of free BUD via the peripheral respiratory tract regions, while a much slower underlying absorption process, attributed to absorption of the drug from the central airways and the formation of BUD fatty acid conjugates within the lung, was considered to contribute to the slowly declining phase.

In general, drug absorption from the alveolar space (peripheral lung regions) is often assumed to be fast due to the high local perfusion, the large absorption surface area and the thin diffusion barrier. The moderately lipophilic character of BUD leads to high solubility in human bronchial secretions which in turn implies fast dissolution (within

6 min) and rapid absorption from the peripheral airways [19]. Conversely, in the conducting airways (central lung regions), absorption of inhaled drugs is found to be slower compared to the peripheral regions, due to less perfusion and thicker airway walls [33]. Nevertheless, apart from a delayed absorption of the centrally deposited drug, a reversible fatty acid esterification of BUD within the airways, further contributes to the slowly absorbed fraction. Budesonide esterification process is both rapid (within 5 min) and reversible and greatly increases the lipophilicity and pulmonary retention of the drug. As the intracellular concentration of free BUD decreases, drug esters are hydrolyzed back to their active state providing a slow-release reservoir of free BUD in the lung over a period of several hours [34,35].

Taking into consideration the above physiological parameters, a two-compartment disposition model with two parallel first-order absorption processes (fast and slow) from the lungs was finally chosen for the description of the C-t profiles of inhaled BUD (Fig. 4). In the developed model, the dose of BUD was assumed to be divided into two different fractions deposited in the two kinetically different lung compartments, allowing explicitly for different absorption rate constants for drug absorption.

The estimates of the population PK parameters obtained for the final model, their BSV% and RSE% values are listed in Table 5. A high absorption rate constant was estimated for the rapidly absorbed fraction ($K_{af} = 19.6 \text{ h}^{-1}$), suggesting that lung is an efficient route of systemic absorption of BUD. Besides, the estimated slow absorption rate constant ($K_{as} = 0.11 \text{ h}^{-1}$) accounted for the slowly absorbed fraction. The ratio of the relative fractions of dose absorbed either fast (R_{fast}) or slowly (R_{slow}) through the lungs (z) was equal to 0.27, suggesting that the main fraction of the inhaled dose was slowly absorbed through the lungs. This finding is further supported by previous studies indicating an increased central lung deposition of inhaled BUD from DPI inhalers, especially in asthma patients and reports showing that most of tissue budesonide remains esterified several hours after inhalation [34,36]. Although the underlying processes are much more complicated, the current approach affords a fair approximation of the underlying absorption process based on a numerically robust, parsimonious model along with the right combination of parameters. In any case, the parameters showing the greatest inter-individual variability for BUD were those describing the absorption from lungs, reflecting the great complexity and variability in lung absorption processes.

The derived BUD volumes of distribution for the central and the peripheral compartments were relatively small (Table 5), which is in line with the intermediate lipophilicity of the drug [33] and broadly consistent with previously reported values [37,38]. In addition, the rapid clearance observed in our study further supports previous findings regarding the rapid systemic dilution and the limited nonspecific tissue retention of the intact, non-esterified BUD [19]. The observed small elimination half-life of the drug following inhalation also minimizes the possibility of 'flip-flop kinetics'. Indeed, many single- and repeated-dose PK studies after intravenous and inhaled administrations of BUD have confirmed the absence of difference in plasma kinetics between these two routes [35].

Finally, the impact of several covariates on the estimated PK parameters was also examined in the case of BUD. Only gender was found to significantly influence K_{as} ($p = 1.6 \times 10^{-5} < 0.05$) and the peripheral volume of distribution V_p/F ($p = 0.00031 < 0.05$) (Table 5), with men showing higher K_{as} values and lower peripheral volumes of distribution compared to female subjects. There is little available information about gender effects on pharmacokinetics, particularly regarding lung absorption of inhaled drugs. The gender effect observed on K_{as} , in our case, might be attributed to a difference in total and regional lung deposition patterns between males and females and other anatomical and dynamic differences. For instance, the size of the lung is found to be larger in men compared to women, particularly in the upper and large conducting airways, offering a wider absorption surface in the more central lung regions [39]. The effect of gender on peripheral

volume of distribution is also in line with the lipophilic character of the drug. The higher body fat percentage in women compared to men may account for the observed higher peripheral volume of distribution of BUD in women. Nevertheless, since inhaled BUD reaches the site of action before it is absorbed systemically, it is not expected that these inter-gender differences will be accompanied by differences in the onset or intensity of therapeutic effect. No other covariate effect (weight, age, height, BMI, FEV1, asthma state, treatment and period) was observed for BUD pharmacokinetics.

5. Conclusions

The aim of the present study was to investigate the absorption and disposition kinetics of FOR and BUD in asthma patients, following a combined inhaled administration using two different dry powder inhalers. Initially, the application of a classic non-compartmental analysis and the subsequent BE assessment, allowed for the estimation of some basic PK parameters and showed the equivalence of the two inhalation products regarding the primary PK parameters for both agents (FOR and BUD). However, this study focused on the population PK analysis of the two inhaled drugs. In case of inhaled FOR, a PK model describing the enterohepatic re-circulation process of the drug was developed in asthma patients. For inhaled BUD, the incorporation of two parallel first-order absorption rate constants (fast and slow) for lung absorption

in the PK model emphasized the importance of pulmonary anatomical features and underlying physiological processes during model development of inhaled drugs. Finally, men were found to exert higher values for the slow absorption rate constant of BUD and smaller peripheral volume of distribution compared to women.

Conflicts of interest

None.

Funding

The research did not receive any specific grant from funding agencies in the public, commercial, or not-for-profit sectors.

Acknowledgements

We wish to thank Elpen Pharmaceutical Co, Greece for providing us all necessary data to perform this computational analysis.

The clinical and bioanalytical parts of the study were commissioned to 3S-Pharmacological Consultation and Research, Germany (Dr S. Rizea Savu clinical part coordination and Dr. L. Silvestro analytical part coordination). The clinical and bioanalytical parts were funded by Elpen Pharmaceutical Co, Greece.

APPENDIX

Table A1

Bioequivalence results for formoterol administered via two different dry powder inhalers (PULMO and SYMBI).

Pharmacokinetic parameters	GMR(%) ^a	Lower 90% CI ^b	Upper 90% CI ^b	Statistical power (%) ^c
AUC _t (pg/mL/h)	96.62	93.46	99.89	100.00
C _{max} (pg/mL)	98.38	91.10	106.24	99.89

^a GMR refers to the geometric mean ratio of the test over reference pharmacokinetic metric.

^b The 90% confidence interval (CI) around the GMR.

^c Statistical power of the study computed using: the estimated GMR, the residual error of the study, level of significance 5%, a number of 90 subjects, and a 2x2 clinical design.

Table A2

Bioequivalence results for budesonide administered via two different dry powder inhalers (PULMO and SYMBI).

Pharmacokinetic parameters	GMR(%) ^a	Lower 90% CI ^b	Upper 90% CI ^b	Statistical power (%) ^c
AUC _t (pg/mL/h)	89.78	83.18	96.90	99.90
C _{max} (pg/mL)	91.30	84.01	99.22	99.68

^a GMR refers to the geometric mean ratio of the test over reference pharmacokinetic metric.

^b The 90% confidence interval (CI) around the GMR.

^c Statistical power of the study computed using: the estimated GMR, the residual error of the study, level of significance 5%, a number of 90 subjects, and a 2 × 2 clinical design.

References

- [1] M. Cazzola, M.G. Matera, Emerging inhaled bronchodilators: an update, *Eur. Respir. J.* 34 (3) (2009) 757–769.
- [2] M. Latorre, F. Novelli, B. Vagaggini, F. Braido, A. Papi, A. Sanduzzi, P. Santus, N. Scichilone, P. Paggiaro, Differences in the efficacy and safety among inhaled corticosteroids (ICS)/long-acting beta2-agonists (LABA) combinations in the treatment of chronic obstructive pulmonary disease (COPD): role of ICS, *Pulm. Pharmacol. Ther.* 30 (2015) 44–50.
- [3] M. Cazzola, M.G. Matera, G. Santangelo, A. Vinciguerra, F. Rossi, G. D'Amato, Salmeterol and formoterol in partially reversible severe chronic obstructive pulmonary disease: a dose-response study, *Respir. Med.* 89 (5) (1995) 357–362.
- [4] S.J. Szefer, Pharmacodynamics and pharmacokinetics of budesonide: a new nebulized corticosteroid, *J. Allergy Clin. Immunol.* 104 (1999) S175–S183.
- [5] H. Derendorf, R. Nave, A. Drollmann, F. Cerasoli, W. Wurst, Relevance of pharmacokinetics and pharmacodynamics of inhaled corticosteroids to asthma, *Eur. Respir. J.* 28 (2006) 1042–1050.
- [6] N. Grekas, K. Athanassiou, K. Papataxiarchou, S. Rizea Savu, L. Silvestro, Pharmacokinetic study for the establishment of bioequivalence of two inhalation treatments containing budesonide plus formoterol, *J. Pharm. Pharmacol.* 66 (12) (2014) 1677–1685.
- [7] R. Donnelly, J.P. Seale, Clinical pharmacokinetics of inhaled budesonide, *Clin. Pharmacokinet.* 40 (6) (2001) 427–440.
- [8] M. Jendbro, C.-J. Johansson, P. Strandberg, H. Falk-Nilsson, S. Edsbäcker, Pharmacokinetics of budesonide and its major ester metabolite after inhalation and intravenous administration of budesonide in the rat, *Drug Metab. Dispos.* 29 (2001) 769–776.

- [9] J.B. Lecaillon, G. Kaiser, M. Palmisano, J. Morgan, G. Della Cioppa, Pharmacokinetics and tolerability of formoterol in healthy volunteers after a single high dose of Foradil dry powder Inhalation via aerolizer™, *Eur. J. Clin. Pharmacol.* 55 (1999) 131–138.
- [10] M.G.M. Derks, B.T.J. van den Berg, J.S. van der Zee, M.C. Braat, C.J. van Boxtel, Biphasic effect-time courses in man after formoterol inhalation: eosinopenic and hypokalemic effects and inhibition of allergic skin reactions, *JPET* 283 (1997) 824–832.
- [11] GINA, Global Initiative for Asthma. A Pocket Guide for Physicians and Nurses, (2009).
- [12] EMA, European Medicines Agency, Guideline on the Investigation of Bioequivalence, (2010) Doc. Ref.: CPMP/EWP/QWP/1401/98 Rev. 1/Corr **. London, 20 January 2010.
- [13] K. Soulele, P. Macheras, L. Silvestro, S. Rizea Savu, V. Karalis, Population pharmacokinetics of fluticasone propionate/salmeterol using two different dry powder inhalers, *Eur. J. Pharm. Sci.* 80 (2015) 33–42.
- [14] K. Soulele, P. Macheras, V. Karalis, Pharmacokinetic analysis of inhaled salmeterol in asthma patients: evidence from two dry powder inhalers, *Biopharm. Drug Dispos.* 38 (2017) 407–419.
- [15] C. Fradette, J. Jean Lavigne, D. Waters, M.P. Ducharme, The utility of the population approach applied to bioequivalence in patients. Comparison of 2 formulations of cyclosporine, *Ther. Drug Monit.* 27 (2005) 592–600.
- [16] Symbicort, Summary of Product Characteristics, Symbicort Turbuhaler 400/12, Inhalation Powder, AstraZeneca UK Limited, 2016.
- [17] B. Weber, G. Hochhaus, A pharmacokinetic simulation tool for inhaled corticosteroids, *AAPS J.* 15 (1) (2013) 159–171.
- [18] C. Mobley, G. Hochhaus, Methods used to assess pulmonary deposition and absorption of drugs, *Drug Discov. Today* 6 (7) (2001) 367–375 1.
- [19] S. Edsbäcker, C.J. Johansson, Airway selectivity: an update of pharmacokinetic factors affecting local and systemic disposition of inhaled steroids, *Basic Clin. Pharmacol. Toxicol.* 98 (2006) 523–536.
- [20] C. Cote, J.L. Pearle, A. Sharafkhaneh, S. Spangenthal, Faster onset of action of formoterol versus salmeterol in patients with chronic obstructive pulmonary disease: a multicenter, randomized study, *Pulm. Pharmacol. Ther.* 22 (1) (2009) 44–49.
- [21] G. Hochhaus, S. Horhota, L. Hendeles, S. Suarez, J. Rebello, Pharmacokinetics of orally inhaled drug products, *AAPS J.* 17 (3) (2015) 769–775.
- [22] D. Al-Numani, P. Colucci, M.P. Ducharme, Rethinking bioequivalence and equivalence requirements of orally inhaled drug products, *AJPS* 10 (2015) 461–471.
- [23] J. Rosenborg, P. Larsson, K. Tegnér, G. Hallström, Mass balance and metabolism of [(3H)]Formoterol in healthy men after combined i.v. and oral administration-mimicking inhalation, *Drug Metab. Dispos.* 27 (10) (1999) 1104–1116.
- [24] H. Sasaki, H. Kamimura, Y. Shiobara, Y. Esumi, M. Takaichi, T. Yokoshima, Disposition and metabolism of formoterol fumarate, a new bronchodilator, in rats and dogs, *Xenobiotica* 12 (1982) 803–812.
- [25] S. Cremers, R. Schoemaker, E. Scholten, J. den Hartigh, J. König-Quartel, E. van Kan, L. Paul, J. de Fijter, Characterizing the role of enterohepatic recycling in the interactions between mycophenolate mofetil and calcineurin inhibitors in renal transplant patients by pharmacokinetic modelling, *Br. J. Clin. Pharmacol.* 60 (3) (2005) 249–256.
- [26] T. Funaki, Enterohepatic circulation model for population pharmacokinetic analysis, *J. Pharm. Pharmacol.* 51 (1999) 1143–1148.
- [27] T.H. Kim, S. Shin, C.B. Landersdorfer, Y.H. Chi, S.H. Paik, J. Myung, R. Yadav, S. Horkovics-Kovats, J.B. Bullitta, B.S. Shin, Population pharmacokinetic modeling of the enterohepatic recirculation of fimasartan in rats, dogs, and humans, *AAPS J.* 17 (5) (2015) 1210–1223.
- [28] T. Wajima, Y. Yano, T. Oguma, A pharmacokinetic model for analysis of drug disposition profiles undergoing enterohepatic circulation, *J. Pharm. Pharmacol.* 54 (7) (2002) 929–934.
- [29] Y.C. Luiking, T.L. Peeters, M.F.J. Stolk, V.B. Nieuwenhuijs, P. Portincasa, I. Depoortere, G.P. van Berge Henegouwen, L.M. Akkermans, Motilin induces gall bladder emptying and antral contractions in the fasted state in humans, *Gut* 42 (1998) 830–835.
- [30] T.C. Northfield, A.F. Hofmann, Biliary lipid output during three meals and an overnight fast. I. Relationship to bile acid pool size and cholesterol saturation of bile in gallstone and control subjects, *Gut* 16 (1) (1975) 1–11.
- [31] J. Behar, Physiology and pathophysiology of the biliary tract: the gallbladder and sphincter of Oddi - a review, *ISRN Physiol.* (2013) 83763015.
- [32] B.T. van den Berg, M.G. Derks, M.G. Koolen, M.C. Braat, J.J. Butter, C.J. van Boxtel, Pharmacokinetic/pharmacodynamic modelling of the eosinopenic and hypokalemic effects of formoterol and theophylline combination in healthy men, *Pulm. Pharmacol. Ther.* 12 (3) (1999) 185–192.
- [33] J.M. Borghardt, B. Weber, A. Staab, C. Kloft, Pharmacometric models for characterizing the pharmacokinetics of orally inhaled drugs, *AAPS J.* 17 (4) (2015) 853–870.
- [34] R. Brattsand, A. Miller-Larsson, The role of intracellular esterification in budesonide once-daily dosing and airway selectivity, *Clin. Ther.* 25 (2003) C28–C41.
- [35] S. Edsbäcker, R. Brattsand, Budesonide fatty-acid esterification: a novel mechanism prolonging binding to airway tissue. Review of available data, *Ann. Allergy Asthma Immunol.* 88 (2002) 609–616.
- [36] K.I. van den Brink, M. Boorsma, A.J. Staal-van den Brekel, S. Edsbäcker, E.F. Wouters, L. Thorsson, Evidence of the in vivo esterification of budesonide in human airways, *Br. J. Clin. Pharmacol.* 66 (1) (2008) 27–35.
- [37] L. Thorsson, S. Edsbäcker, A. Källén, C.G. Löfdahl, Pharmacokinetics and systemic activity of fluticasone via Diskus and pMDI, and of budesonide via Turbuhaler, *Br. J. Clin. Pharmacol.* 52 (5) (2001) 529–538.
- [38] M. Hübner, G. Hochhaus, H. Derendorf, Comparative pharmacology, bioavailability, pharmacokinetics, and pharmacodynamics of inhaled glucocorticosteroids, *Immunol. Allergy Clin. North Am.* 25 (3) (2005) 469–488.
- [39] C.S. Kim, S.C. Hu, Regional deposition of inhaled particles in human lungs: comparison between men and women, *J. Appl. Physiol.* 84 (6) (1998) 1834–1844 (1985).